ORIGINAL ARTICLE

Magnetic resonance imaging based computer-guided dental implant surgery—A clinical pilot study

Florian Andreas Probst MD, DMD, PhD[1] | Josef Schweiger MSc[2] |
Maria Juliane Stumbaum DMD[2] | Dimitrios Karampinos PhD[3] |
Egon Burian MD, DMD[4] | Monika Probst MD[4]

[1]Department of Oral and Maxillofacial Surgery and Facial Plastic Surgery, University Hospital, LMU Munich, Munich, Germany

[2]Department of Prosthetic Dentistry, University Hospital, LMU Munich, Munich, Germany

[3]Department of Diagnostic and Interventional Radiology, Klinikum rechts der Isar, Technical University Munich, Munich, Germany

[4]Department of Diagnostic and Interventional Neuroradiology, Klinikum rechts der Isar, Technical University Munich, Munich, Germany

Correspondence
Florian Andreas Probst, MD, DMD, PhD, Department of Oral and Maxillofacial Surgery and Facial Plastic Surgery, University Hospital, LMU Munich, Lindwurmstr. 2a, 80337 Munich, Germany.
Email: florian.probst@med.uni-muenchen.de; flo.probst@web.de

Abstract

Background: Computer-guided implant surgery is currently based on radiographic techniques exposing patients to ionizing radiation.

Purpose: To assess, whether computer-assisted 3D implant planning with template-guided placement of dental implants based on magnetic resonance imaging (MRI) is feasible.

Materials and methods: 3-Tesla MRI was performed in 12 subjects as a basis for prosthetically driven virtual planning and subsequent guided implant surgery. To evaluate the transferability of the virtually planned implant position, deviations between virtually planned and resulting implant position were studied. Matching of occlusal surfaces was assessed by comparing surface scans with MRI-derived images. In addition, the overall image quality and the ability of depicting anatomically important structures were rated.

Results: MRI-based guided implant surgery with subsequent prosthetic treatment was successfully performed in nine patients. Mean deviations between virtually planned and resulting implant position (error at entry point 0.8 ± 0.3 mm, error at apex 1.2 ± 0.6 mm, angular deviation 4.9 ± 3.6°), mean deviation of occlusal surfaces between surface scans and MRI-based tooth reconstructions (mean 0.254 ± 0.026 mm) as well as visualization of important anatomical structures were acceptable for clinical application.

Conclusion: Magnetic resonance imaging (MRI) based computer-assisted implant surgery is a feasible and accurate procedure that avoids exposure to ionizing radiation.

KEYWORDS
CAD/CAM, computer-assisted surgery, guided implant surgery, implant dentistry, magnetic resonance imaging (MRI), oral and maxillofacial surgery, virtual surgical planning

1 | INTRODUCTION

X-ray-based three-dimensional (3D) imaging, in particular cone beam computed tomography (CBCT), has become established for presurgical planning in implant dentistry.[1] In addition to the diagnosis of various pathologies, CBCT serves to evaluate relevant anatomical structures such as the mandibular canal, maxillary sinus, or teeth. Beyond that, CBCT is increasingly used as the imaging modality of choice for virtual surgical planning and subsequent fabrication of CAD/CAM (computer-aided design and computer-aided manufacturing) fabricated surgical guides, also called guided implant surgery.[1,2] Dedicated planning software enables virtual implant positioning that primarily follows the prosthetic requirements but also considers anatomical aspects. Static guidance systems in the form of drilling guides transfer the virtually planned implant position to the surgical site within a clinically reasonable level of accuracy.[2-4]

However, CBCT exposes patients to a relevant amount of ionizing radiation with associated cancer risk.[5,6] This should be viewed particularly critically in the context of otherwise healthy patients and elective surgery. Even assuming that the risk to individuals is low, radiation exposure from CBCT is certainly relevant seen from a public health perspective.[7] Another drawback of CBCT with regard to planning in implant dentistry is that tracing of the inferior alveolar nerve can be difficult in the absence of a well corticated mandibular canal.[8]

Magnetic resonance imaging (MRI) may serve as an alternative imaging modality in implant dentistry. Some earlier clinical studies have shown that MRI data can, in principle, serve as a basis for implant planning, however, without considering the aspect of guided implant surgery.[9-12] 3D isotropic resolution MRI sequences (eg, 3D T1-weighted Black Bone Sequences) at the latest 3 Tesla (3 T) MRI scanners using dedicated coils currently enable dental imaging with significant increase in resolution, improvement of the signal-to-noise ratio, reduction in acquisition times as well as artifact suppression.[13-18] With regard to the measurement of bony dimensions, a good agreement between CBCT and MRI was described.[13,19-21] Also, the CAD construction of virtual 3D models of craniofacial bone in STL format (STL = standard triangulation/tessellation language) based on MRI data has been evaluated,[22] which is a basic requirement for integration of MRI data into the workflow of computer-assisted surgery planning. By superimposing MRI-derived 3D models of the jaw and corresponding digitalized information that precisely represent tooth surfaces, it is ultimately possible to generate detailed hybrid models, which serve as the basis for CAD/CAM fabrication of surgical guides. As a result, MRI is increasingly becoming the focus of attention as a diagnostic basis for implant planning.[23,24] One recently published case report demonstrates a proof-of principle of template-guided implant placement based on MRI.[25] So far, there is no research testing feasibility of this approach with special regards to accuracy of implant placement. In addition to eliminating exposure to ionizing radiation, MRI scans also promise potential diagnostic value over CBCT or computed tomography (CT) because of its superior soft tissue contrast. This makes it possible to directly visualize neurovascular structures such as the inferior alveolar nerve or the dental pulp.[8,18,26-28]

For the reasons set out above, the aim of this study was to show if computer-assisted 3D implant planning with template-guided placement of dental implants carried out based on MRI-derived data is feasible.

2 | MATERIAL AND METHODS

2.1 | Study design

The investigators designed and implemented a retrospective single-center pilot study.

The study sample was derived from a patient population undergoing treatment from January 2018 to June 2019 in the Department of Oral and Maxillofacial Surgery and Facial Plastic Surgery and in the Department of Prosthetic Dentistry, University Hospital, LMU Munich, Germany. Subjects eligible for study inclusion underwent MR imaging for presurgical planning of dental implant treatment. The institutional ethics committee approved the retrospective study protocol (approval number 19-432).

2.2 | Magnetic resonance imaging

Thermoformed splints of 1.5 mm thickness (Scheu-Dental, Iserlohn, Germany) that have the basic shape of an impression tray were produced on the basis of individual model casts. The splints were filled with hydrocolloid gel (Systoloid universal green, American Dental Systems, Vaterstetten, Germany), a reversible thermoplastic impression material, and placed on the model casts. After the hydrocolloid gel had hardened, it was removed together with the splint. Finally, the splints containing the solid hydrocolloid, which served as local contrast providing material, were placed intraorally on the corresponding jaw during the MRI examination to improve delineation of the tooth surfaces.

All patients included in the study underwent MRI on a 3 T system (Elition, Philips Healthcare, Best, the Netherlands) using a 16-channel Head and Neck Spine array, which was placed on top of the head. Patients were positioned head-first in a supine position. A high isotopic-resolution 3D T1-weighted sequence was used for optimized bone visualization. Partial Fourier imaging with a factor of 60% was employed in the 3D T1-weighted sequence to reduce the echo time.[29] Additionally, a 3D T2-weighted short tau inversion recovery (STIR) sequence was performed for the improved representation of soft tissues, in particular to depict the inferior alveolar nerve. These sequences represent standard MRI sequences and are commonly used in clinical practice. Sequence specifications for 3D T1-weighted bone and 3D T2-weighted STIR sequence are listed in Table 1. The primary orientation used for data acquisition was axial for the 3D T1-weighted and the 3D T2-weighted STIR sequence. Given the employed isotropic voxel size, the 3D T1-weighted sequence images could be reformatted in all planes.

TABLE 1 Specifications of MRI sequences

3D T1-weighted bone sequence	
Acquisition time	03:08 min
FOV	180 mm
Matrix	420 × 419
Acq voxel	0.6 × 0.6 × 0.6 mm^3
Number of signal averages	1
TR	10 ms
TE	1.75 ms
CS-SENSE	yes
reduction	2.3
WFS (pix)/bandwidth (Hz)	1503/289
3D T2-weighted STIR sequence	
Acquisition time	06:03 minutes
FOV	200 mm
Matrix	308 × 308
Acq voxel	0.65 × 0.65 × 1 mm^3
Number of signal averages	1
TR	2300 ms
TE	184 ms
IR	250 ms
Slice oversample factor	1.5
CS-SENSE	yes
reduction	5
WFS (pix)/bandwidth (Hz)	1766/246

Note: 3D T1-weighted bone sequence and 3D T2-weighted STIR sequence.

2.3 | Virtual planning, additive manufacturing, and guided surgery

The clinical workflow for MRI-based computer-guided implant surgery is illustrated in Figures 1-3. DICOM (digital imaging and communications in medicine) MRI data (3D T1-weighted bone sequence) as well as digitalized occlusal information (tooth surfaces), obtained either by dental model scans or intraoral scans, were imported into a dedicated implant planning software (3Shape Implant Studio, 3Shape, Copenhagen, Denmark). At first, occlusal surface data were superimposed on the MRI-derived volume data. The alignment was fine-tuned in the coronal, axial, and sagittal plane using translation and rotation tools to obtain accurate matching resulting in a "Hybrid-Model" (Figure 1). Next, the implant position was set following prosthetic requirements and considering the anatomic situation. To achieve an exact prosthetic target definition, a digital set-up of the planned restoration was created using CAD tools. The planning software then automatically suggested a preliminary implant position based on the position and axes of the digital set-up. Subsequently, the implant position was adapted to anatomical criteria, such as bone availability, mandibular canal, maxillary sinus, and so on, and finalized (Figure 2).

After the CAD construction of a drilling guide (Figure 3), the generated STL data were prepared for 3D printing with CAM software (BEGO CAMCreator, BEGO Medical, Bremen, Germany). The additive manufacturing process was carried out on a 3D printer (BEGO Varseo, BEGO Medical, Bremen, Germany) using digital light processing (DLP process). After printing, the 3D-print was cleaned in isopropanol, the support structures were removed and the surfaces smoothed. After gluing in of titanium guide sleeves, the manufacturing process of the rigid drilling guide was completed.

Using the drilling guides, a fully guided drilling sequence was performed according to the implant manufacturer's specifications (Straumann Guided Surgery, Straumann AG, Basel, Switzerland and CamlogGuide, Camlog, Basel, Switzerland) prior to final implant placement (Figure 3).

2.4 | Study variables, data acquisition, and analysis

To study the feasibility of the MRI-based approach, it was reviewed from a clinical point of view, whether MR images were suitable for the virtual planning and if a surgically and prosthetically adequate implant position was ultimately achieved. For a more accurate and objective analysis, the deviations between virtually planned and the finally resulting implant position were analyzed as follows. Master casts that had been routinely made for the fabrication of the final restoration were employed for this purpose. Individual trays and polyether were used for the analogue impression of teeth and implants. Impression posts were screwed on the implants before taking the impression with an open impression tray. Lab-analogues were inserted into the impression posts and then the master casts were made with stone plaster class 4 (Resinrock, Whipmix, Louisville, Kentucky). After fabrication of the master casts, implant scanbodies were fixed on the lab-analogues and scanned with an optical structured-light scanner (S900, Zirkonzahn, Gais, Italy). The digitalized master casts with implant scan bodies were matched to exported STL-files representing the virtual planning and deviations of implant positions were finally measured by 3-matic (Materialise, Leuven, Belgium). In two cases, due to a complete digital prosthetic workflow, no master cast were available. Therefore, the postoperative implant position was detected with an intraoral scanning device (CEREC Omnicam, Dentsply Sirona, York). Outcome variables were set according to Tahmaseb and colleagues 2018,[2] evaluating the deviation at entry point and at apex location (mm) as well as the angular deviation (degree) (Figure 4). These metrically assessed deviations between virtually planned and the finally resulting implant position were defined as primary outcome variables.

As secondary outcome variables, matching between occlusal surfaces of 3D scans of stone models and occlusal surface reconstructions derived from MRI data was assessed. For this purpose, the practicability of aligning occlusal tooth surface data and MRI data in the coronal, axial and sagittal planes was assessed first (Figure 1). Therefore, cases were reviewed in the planning software and the degree of two-dimensional matching between the scanned occlusal data and MRI-derived volume data was rated on a five point Likert
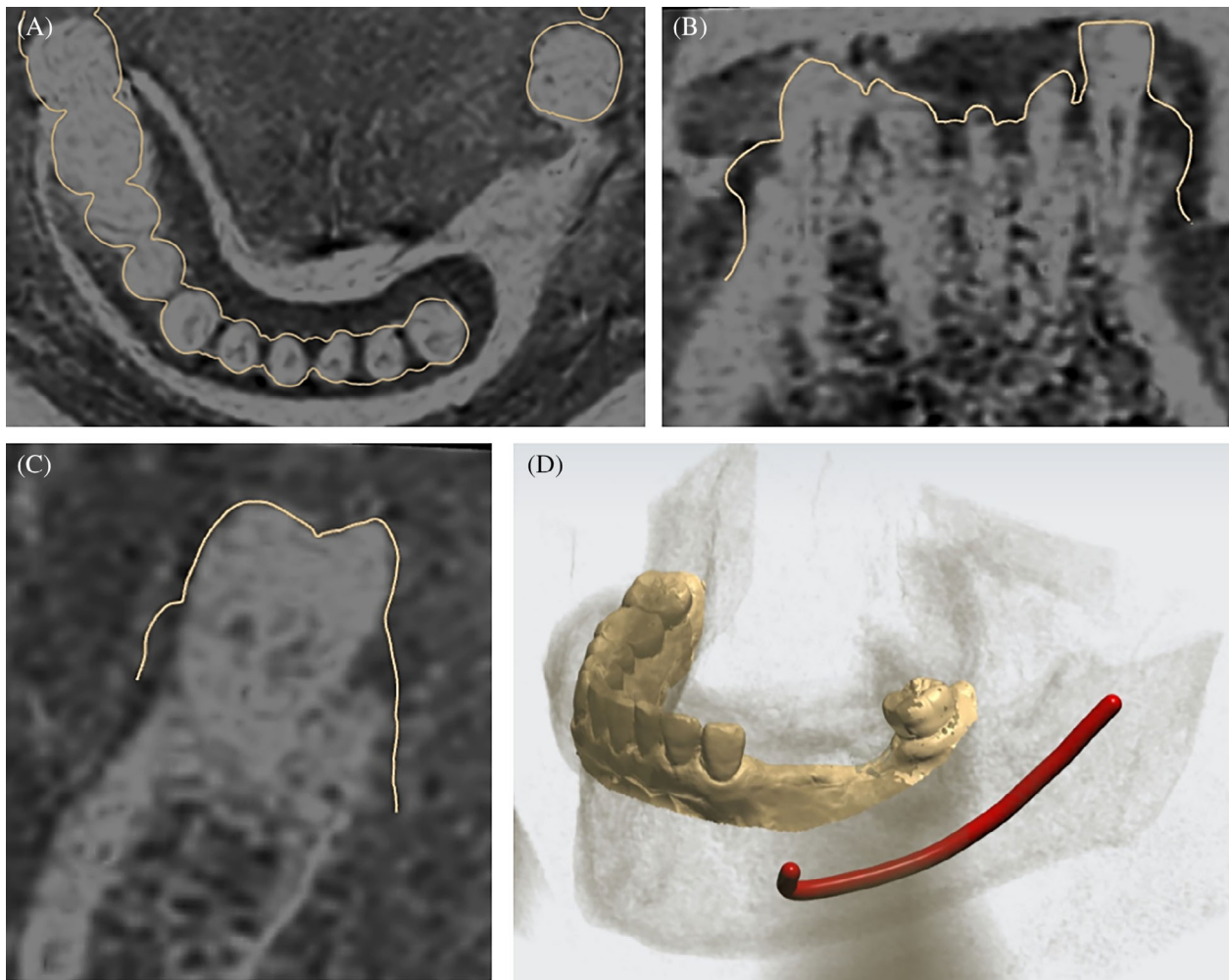
FIGURE 1 Top and Bottom left: Digitalized occlusal surfaces derived from a model scan (beige lines) are superimposed with MRI DICOM data in the planning software. The alignment is fine-tuned in the coronal, axial and sagittal planes using translation and rotation tools to achieve an exact matching. Please note: In this case, the signal values of the T1-weighted images were previously inverted (black to white) to provide a CBCT-like appearance. Bottom right: Resulting 3D "Hybrid Model" with the traced inferior alveolar nerve (displayed in red)

scale (1 = extremely poor matching, not clinically applicable, 2 = poor matching, clinical use is not advised, 3 = average matching, borderline clinical use, 4 = good matching, containing no substantial adverse effect for clinical use, 5 = excellent matching, no restrictions for clinical use). Ratings were made in agreement with a dental technician and oral and maxillofacial surgeon each with approximately 10 years of experience concerning computer-guided implant surgery. Then, for metrical evaluation, tooth crowns and especially occlusal structures represented in the MR images were segmented with Mimics (Materialise, Leuven, Belgium) in analogy to an algorithm applied to CBCT data reported by Sang and colleagues 2016,[30] exported to an STL-file (.stl) and matched with the corresponding surface scans using the software 3-matic (Materialise, Leuven, Belgium). Unsigned geometric deviations of occlusal surfaces between model scans and MRI-derived occlusal reconstructions concerning complete or partial dental arches were measured (Figure 5). In case of severe artifacts due to metallic restorations, single teeth were excluded from matching.

Further secondary outcome variables were introduced to evaluate the ability of MRI to image important anatomical structures in the context of guided implant surgery. In particular, cortical bone, spongious bone, teeth, maxillary sinus, and the mandibular canal were assessed in the 3D T1-weighted bone sequence, the inferior alveolar nerve was assessed in the 3D T2-weighted STIR sequence. Additionally, image quality was judged taking motion and susceptibility artifacts into account (Table 2). Rating was performed on a five point Likert scale (1 = extremely poor, images are not clinically useful, 2 = poor, clinical use is not advised, 3 = average, borderline clinical use due to the image quality, 4 = good, containing no substantial adverse effect for clinical use, 5 = excellent, no restrictions for clinical use). Ratings were made in agreement with a senior radiologist with experience in head and neck imaging and an oral and maxillofacial surgeon, both with more than 10 years of professional experience.

Further study variables include demographic data, region of implant placement, support of drilling guide (tooth-supported/mucosa-supported), fitting of surgical guides, intra- and postoperative complications, and need for revision surgery (yes/no). In addition, the average number of metallic restorations per jaw and the average number of teeth excluded for the metrical matching analysis (deviations from surface scans with MRI-based tooth reconstructions) due to metallic artifacts were recorded.
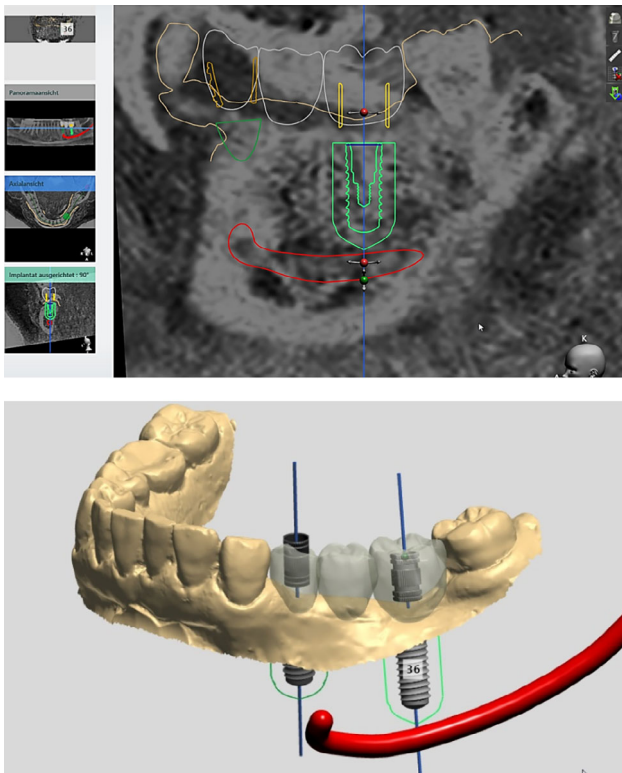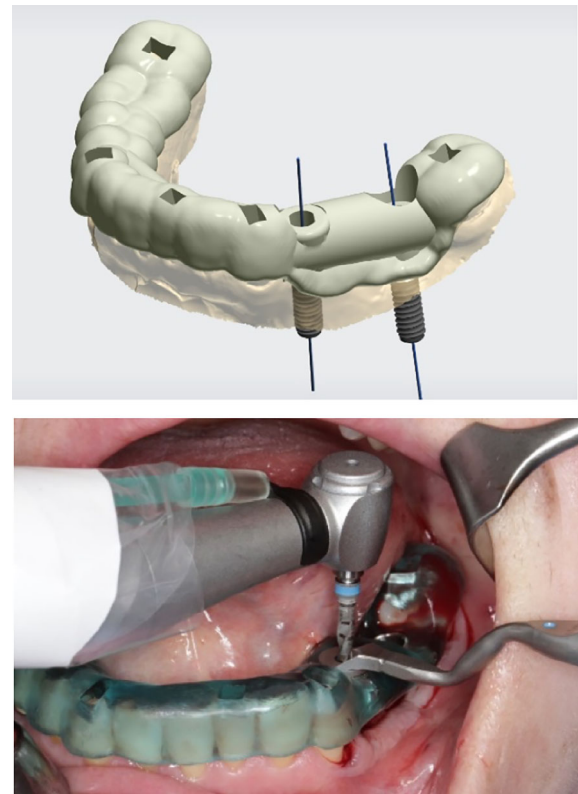
FIGURE 2 Top: Virtual positioning of an implant in region 36 in parasagittal section according to prosthetic requirements. Bottom: 3D view of the virtually positioned implants in region 34 and 36 in relation to the digital set-up of the planned dental restoration and to the traced inferior alveolar nerve

FIGURE 3 Top: CAD construction of a rigid drilling guide. Bottom: Surgery with fully guided implant drilling sequence in the left mandible

Statistical analysis was carried out with SPSS 24 (SPSS Inc., Chicago, Illinois). Descriptive statistics were performed for each study variable. 95% confidence intervals (CI) were provided for metrically assessed variables.

3 | RESULTS

The study sample included 12 subjects (7 female, 5 male), patients' mean age at time of MR-imaging was 48.6 ± 16.6 years.

One patient showed pronounced susceptibility artifacts due to multiple and large-dimensioned titanium plates after bimaxillary orthognathic surgery (Likert rating 2 = poor, clinical use is not advised, Table 2). In another patient, the overall image quality of the MRI was compromised by motion artifacts (Likert rating 3 = average, borderline clinical use due to the image quality, Table 2). In these two cases, guided-surgery was finally performed on the basis of CBCT data instead. Moreover, an additional implant treatment was postponed at the patient's request and solely radiological data and matching between MRI-derived and scan-derived tooth surfaces were evaluated. In 9 out of 12 patients, a total of 12 implants were finally inserted using MRI-based guided implant surgery, with a fully guided drilling sequence in 8 cases (n = 11 implants) and a pilot-drill guided implant placement in one single case (n = 1 implant). Twelve implants

were inserted in 10 partially edentulous jaws (in one patient implants were placed on both maxilla and mandible) in the premolar (n = 6) or molar (n = 6) region either of the maxilla (n = 6) or mandible (n = 6).

In each jaw, no more than two single prosthetic restorations were intended, either in form of an implant-supported single crown or bridge. No intra- and postoperative complications and no need for revision surgery were recorded. Drilling guides were either completely tooth-supported (n = 7) or mainly tooth-supported (n = 3, unilateral free-end situations in the molar region). Intraoperatively, there was a very good fitting of all surgical guides (n = 10/10; in one patient implants were inserted in the maxilla and mandible). Orienting intraoperative assessment of implant position with a depth gauge as well as postoperative panoramic imaging showed satisfying angulation in all cases (n = 12/12 inserted implants). In all patients, the prosthetic restoration was successfully finished and inserted.

The mean deviation at entry point and at apex location was 0.8 ± 0.3 mm (n = 11, range 0.4-1.2 mm, 95% CI 0.6-0.9 mm), and 1.2 ± 0.6 mm (n = 11, range 0.5-2.3 mm, 95% CI 0.8-1.6 mm) and the mean angular deviation between virtual vs resulting implant position was 4.9 ± 3.6° (n = 11, range 1.2-14.6°, 95% CI 2.5-7.3°) (Figure 4).

The practicability of alignment between surface scans and MRI-based tooth reconstructions in the planning software was rated from good (Likert rating 4, n = 8/11) to excellent (Likert rating 5, n = 3/11). Mean deviation between occlusal surfaces of model scans and MRI-derived occlusal reconstructions was 0.254 ± 0.026 mm (n = 12, range
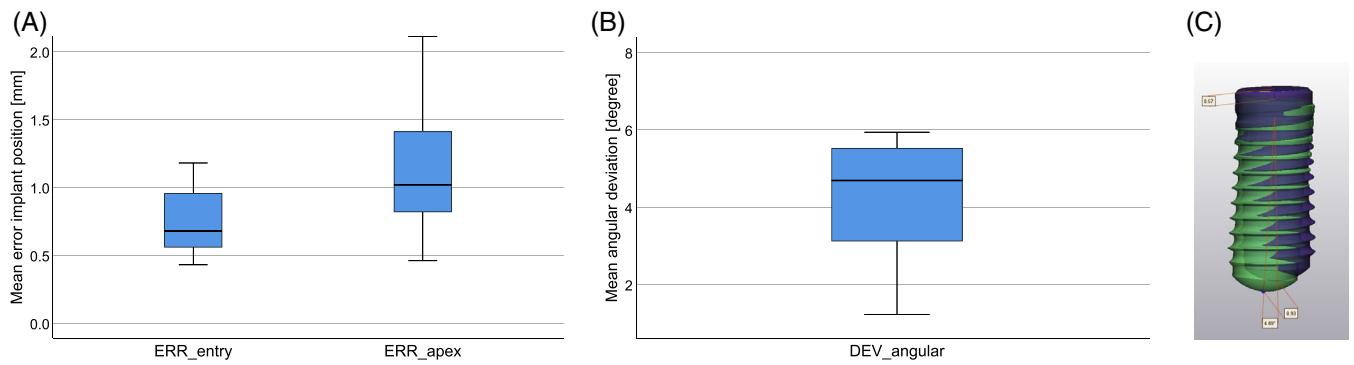
FIGURE 4 Difference between virtually planned and finally resulting implant position. A, Boxplots of mean deviation at entry point (left, ERR_entry) and at apex location (right, ERR_apex) of 0.8 ± 0.3 mm and 1.2 ± 0.6 mm. B, Mean angular deviation between virtual vs resulting implant position (DEV_angular) of 4.9 ± 3.6°. C, Exemplary image showing virtually planned (colored blue) and resulting (colored green) implant position
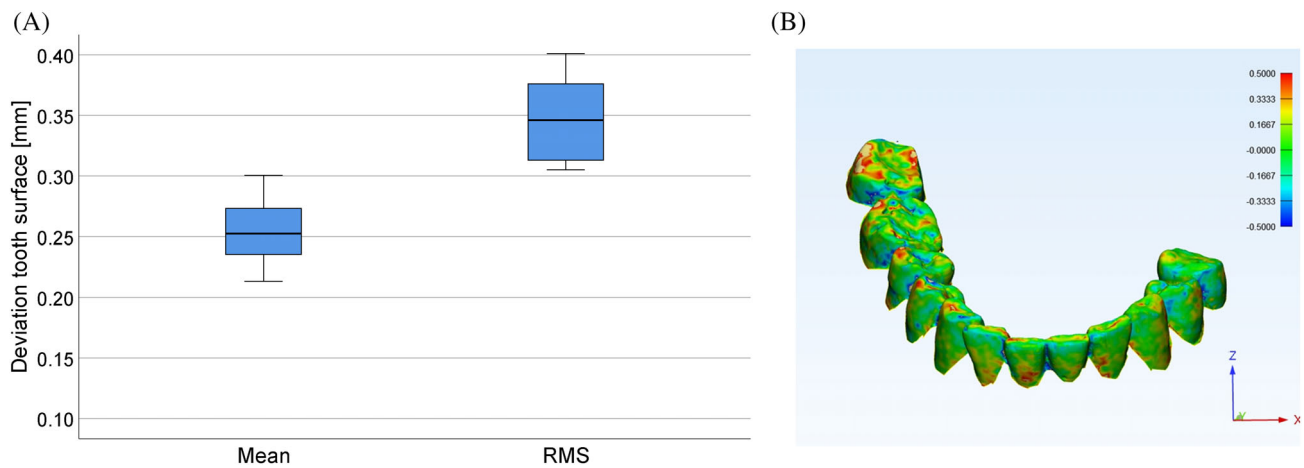
FIGURE 5 Geometric deviations of occlusal surfaces between model scans and MRI-derived occlusal reconstructions. A, Boxplots of mean value (left) 0.254 mm ± 0.026 mm and root mean square (RMS) value (right) 0.347 ± 0.034 mm. B, Color mapping showing distribution of geometric deviations (limits set from −0.5 to +0.5 mm) of a MRI-derived occlusal reconstruction compared to occlusal surface of corresponding model scan in a sample patient

TABLE 2 Radiological evaluation of MR images

	MRI sequence	Rating 1 and 2	Rating 3	Rating 4	Rating 5
Cortical bone	T1 Bone	—	—	—	12
Spongious bone	T1 Bone	—	—	2	10
Teeth	T1 Bone	—	—	2	10
Maxillary sinus	T1 Bone	—	—	2	10
Mandibular canal	T1 Bone	—	3	3	6
Inferior alveolar nerve	T2 STIR	—	—	—	12
Image quality—Motion artifacts	T1 Bone	—	1	2	9
Image quality—Susceptibility artifacts	T1 Bone	1	—	7	4

Note: Quality of visualization of anatomical structures and image quality taking motion and susceptibility artifacts into account. Rating on a five point Likert scale (1 = extremely poor, images are not clinically useful, 2 = poor, clinical use is not advised, 3 = average, borderline clinical use due to the image quality, 4 = good, containing no substantial adverse effect for clinical use, 5 = excellent, no restrictions for clinical use). The numbers in the table reflect the number of patients assigned to the respective rating. T1 Bone = 3D T1-weighted bone sequence, T2 STIR = 3D T2-weighted STIR sequence.

0.213-0.300 mm, 95% CI 0.237-0.271 mm), root mean square (RMS) was 0.347 mm ± 0.034 mm (n = 12, range 0.305-0.401 mm, 95% CI 0.325-0.369 mm) (Figure 5). The RMS values corresponded to 58% of the voxel size (0.6 mm). The average number of metallic restorations per jaw was 5.4 ± 2.5. With regard to the 3D metrical surface matching, an average number of 1.1 ± 1.1 teeth were excluded and averagely 11.6 ± 0.9 teeth remained for the metric occlusal matching procedures.

Using the 3D T1-weighted bone sequence, cortical and spongious bone as well as teeth were clearly visible (Table 2 and Figure 6). This sequence dedicated for visualizing bone is comparable to CBCT imaging. However, the visibility of the mandibular canal was limited, whereas 3D T2-weighted STIR provides direct nerve imaging and offers a diagnostic added value compared to CBCT (Table 2 and Figure 6). Moreover, the maxillary sinus and the border between the sinus and the maxillary alveolar process were well displayed (Table 2). In all cases that were finally selected for guided implant surgery, no adverse effects for clinical use was observed with regard to motion and susceptibility artifacts (Table 2). Susceptibility artifacts due to metallic restorations were limited to the area of the occlusal surfaces and dental crowns and did not affect bony structures, the inferior alveolar nerve, or the maxillary sinus.

FIGURE 6 Top: Parasagittal reconstruction of a 3D T1-weighted bone sequence. This is practically a sequence specialized for bone imaging comparable to CBCT. Cortical and spongious bone as well as teeth are clearly visible. However, the visibility of the mandibular canal is limited. Bottom: 3D T2-weighted STIR sequence functions as a "nerve sequence" during implant planning, which enables direct nerve imaging (yellow arrows are indicating the course of the inferior alveolar nerve) and thus provides a diagnostic added value compared to CBCT

4 | DISCUSSION

The goal of this study was to show if computer-assisted 3D implant planning with template-guided placement of dental implants based on MRI data is a feasible procedure. In all cases where guided implant surgery was performed, MRI-based virtual planning and transfer by static guides with subsequent prosthetic treatment was successfully performed. The deviations between virtually planned implant position and the finally resulting implant position, the deviations of occlusal surfaces between digitalized stone models and MRI-derived occlusal data, and the visualization of important anatomical structures were acceptable for clinical application. Consequently, the MRI-based guided surgery approach was feasible.

MR images displayed all anatomical structures that are relevant for dental implant planning. As has already been demonstrated in other investigations, bone tissue, teeth, and maxillary sinus could be clearly depicted in this study.[13,16,23,25] As the occasional term "black bone MRI" suggests, cortical bone and other tissues with short T_2^* relaxation times including mineralized structures such as teeth initially appear black in T1-weighted bone sequences and results in an unusual imaging impression compared to the one derived from CBCT or CT. However, the dark signal values of the MR-image data sets can be inverted optionally to provide a bright or white impression of tooth structures and cortical bone (Figures 1 and 2), providing the clinical practitioner with a more familiar image impression.[31] It is important to keep in mind that any tissues with short T2* and regions filled with air will also appear bright after the inversion of the signal of the T1-weighted sequence.

In our study, we did not use any dedicated surface coils as described in earlier studies[32] because a good signal-to-noise ratio and a short acquisition time could be achieved without any additional coils. This is mainly due to the good gradient hardware performance of the employed 3 T scanner (Elition, Philips Healthcare) used and the acquisition time reduction made possible by the combination of compressed sensing with sensitivity encoding (SENSE) parallel imaging.[33,34] Sequence parameters were optimized taking into consideration spatial resolution and total image acquisition time requirements. The longer the image acquisition time, the higher the occurrence of motion artifacts. 3D isotropic -voxel size of 0.6 mm³ resulted in an acquisition time of a little more than 3:08 minutes, what appears reasonable in terms of clinical applicability (Table 1). Intraoral surface coils as described by Fluegge and colleagues[13] can generate a very high spatial resolution but they may be not yet approved for clinical use.

Based on the 3D T1-weighted sequence, delineation of the mandibular canal, which is important for implant planning in the posterior mandibular region, succeeded from acceptable to excellent. It is well known that the detection of the mandibular canal and the indirect tracing of the inferior alveolar nerve can be difficult in the absence of a well-corticated mandibular canal or in the presence of motion and metallic artifacts. This applies to both T1-weighted sequences and CBCT imaging.[8] However, MR imaging offers a unique advantage and added value through the application of soft tissue contrasting sequences such as T2-weighted STIR sequences. While the

T1-weighted sequence is practically a "bone sequence" and thus comparable with CBCT imaging, the T2-weighted STIR sequence can function as a "soft tissue & nerve sequence" during implant planning, which enables direct nerve imaging (Figure 6). In the present study, only T1-weighted sequences were integrated into the implant planning software and T2-weighted STIR sequences were examined separately. In future work, the fusion of T1-weighted and T2-weighted sequences and the subsequent import of these merged data into a planning software should be considered.

Motion artifacts can compromise the overall image quality and play a role in MR-imaging as the examination times are significantly increased compared to CT or CBCT.[23] In our study, in one patient, CBCT was preferred for implant planning due to pronounced motion artifacts. In all other patients, no adverse effect for clinical use could be observed, which is possibly due to the relatively short recording time of just over 3 minutes for the 3D T1-weighted sequence. Approaches to reduce motion artifacts may include the use of shorter measurement times, stable positioning of the patient's head and the use and further development of motion correction tools.[35]

Susceptibility artifacts, caused by dental materials, may significantly affect the local assessment of structures when the causative materials are in close proximity. In this study, one patient showed severe susceptibility artifacts through multiple titanium plates in the midface and mandible after orthognathic surgery. In all other patients, more or less pronounced artifacts were seen in metallic dental restorations, although these were essentially limited to the area of the occlusal surfaces and dental crowns. Other anatomical structures such as bone, maxillary sinus, and soft tissues were basically unaffected and implant planning was not impaired. Though artifacts caused by dental materials may be a limiting factor in MRI, this also applies to radiation-based techniques like CT or CBCT and MRI might even be superior to CBCT in terms of these artifacts.[36] Special applications for artifact suppression caused by ferromagnetic materials were not applied in the cases investigated here, but the implementation of artifact reducing applications such as view angle tilting[17,18] is basically possible. However, while some materials such as stainless steel and cobalt-chromium samples are responsible for pronounced artifacts that may no longer allow reasonable diagnostics, the large majority of dental materials such as zirconium dioxide, amalgam, gold alloy, gold-ceramic crowns, titanium alloys, some composites, and nickel-titanium cause only low to moderate artifacts.[37]

In all cases where MRI-based guided implant surgery was performed, a good clinical outcome was evident with regard to occurrence of complications, fitting of surgical guides and indicative intraoperative assessment of implant position with a depth gauge as well as postoperative panoramic imaging. The metric analysis of the planned vs the actual implant position showed clinically acceptable to very good results as well. The mean values for the deviations at entry point (0.8 ± 0.3 mm) and at apex location (1.2 ± 0.6 mm) are lower or fairly accurate to the ranges given in recent reviews and meta-analysis.[2,38] The measured angular deviation (4.9 ± 3.6°) was rather in the upper range of deviations reported. This is due to a single outlier likely caused by eccentric drilling at limited mouth opening and deformation of the drilling guide in a free-end situation.

Imaging data alone do not represent tooth/occlusal surfaces accurately enough to provide a tooth-supported guide.[39] As a basic requirement for template assisted guided implant surgery, however, tooth surfaces should be displayed at least accurately enough to allow superimposition with high-precision scan-based virtual models.[23,40] This pilot series showed that by employing a common planning program, the surface scan models could be registered without practical restrictions with the MRI-based reconstructed tooth surfaces. This was possible under practical conditions with an average of 5 to 6 metallic restorations per jaw. Individual local inaccuracies were well compensated for by superimposing complete or partial dental arches in the sense of a global registration method. 3D comparisons of the deviations between MRI-reconstructed and scan-derived tooth surfaces, carried out for further evaluation of the methodology, showed values (mean deviation 0.254 ± 0.026 mm, RMS value 0.347 ± 0.034 mm) acceptable for clinical application. With regard to tooth surface matching, on average one tooth was excluded and 11 to 12 teeth remained per jaw for the metric occlusal matching procedures, which can be considered a valid representation of the whole dental arch. Based on linear measurements, Flügge et al reported mean deviations between CBCT derived tooth surfaces and model scan derived surfaces of about 0.4 mm after manual CBCT segmentation.[40] A recent study showed that MRI is able to visualize tooth surfaces in-vivo with acceptable accuracy for guided implant surgery planning.[23] Yet, the accuracy was considerably lower compared to CBCT (overall RMS values 0.102 ± 0.042 mm for CBCT and 0.261 ± 0.08 mm for MRI). In comparison, the RMS value of the registration accuracy was higher in our study. This can be explained by the fact that geometric deviations seem to correlate with the resolution of the imaging procedure. RMS values of about 60% of the voxel size were reported for CBCT and MRI.[23,30] This is in accordance with the present study, in which RMS values corresponded to 58% (0.347/ 0.600 × 100%) of the voxel size. In contrast to the study of Hilgenfeld and colleagues[23] and to better reflect the practicability for guided implant surgery, three-dimensional geometric deviations of complete dental arches were determined.

MRI has an obvious advantage compared to CBCT in the context of guided implant surgery because it sufficiently depicts tooth and bone tissue while avoiding any exposure to ionizing radiation. Furthermore, MRI may provide added diagnostic value by the excellent contrast of soft tissues, which allows for example a direct imaging of peripheral nerve tissue such as the inferior alveolar nerve as demonstrated in this study. Such direct nerve visualization may be beneficial for presurgical planning prior to implant dentistry but also prior to other procedures such as wisdom tooth removal or orthognathic surgery.[8,28] Within the context of implant surgery, MRI enables the measurement of mucosal thickness and may help planning of palatal tissue harvesting.[41] MRI may also enable postoperative evaluation of implants[18,19,42] and may offer the opportunity for detecting peri-implant bone defects 3-dimensionally.[36] Further promising innovative application of MRI in dentistry include the differential diagnosis between cystic jaw lesions,[43,44] the evaluation and monitoring of tooth vitality via the signal of the dental pulp[13,15,26] and three-dimensional orthodontic diagnostics.[20,45]

The advantages offered by MRI must ultimately be compared with the corresponding limitations in order to assess the actual potential in computer guided implant surgery. First, difficulties may arise, for example, from motion and susceptibility artifacts, which have already been discussed in the text above. Second, there are some contraindications such as the presence of pacemakers, cochlear implants, or neurostimulators. Third, the MRI-based approach is subject to cost and availability limitations. For instance, some specific sequences for optimized presentation of dental structures are not yet freely available. The acquisition and maintenance costs of MRI devices are considerably higher than for CBCT devices. Therefore, in contrast to CBCT, the possibility of on-site use in dental practice is significantly reduced and dental practitioners would have to cooperate with radiology departments that offer dental MRI applications. Finally, limitations regarding the study design merit mentioning. The study has the known disadvantages associated with a retrospective work and/or a pilot series. This includes for example some minor differences in the clinical workflow and the analysis of the resulting implant positions. In order to better assess the actual accuracy of a MRI-based approach and to be able to compare it with the established CBCT-based planning, a randomized controlled trial is required, building on the promising results of this feasibility study.

5 | CONCLUSIONS

In conclusion, MRI-based computer-assisted implant surgery is a feasible and accurate procedure, eliminating radiation exposure. In addition, MRI provides added diagnostic value through direct visualization of soft tissues such as the alveolar inferior nerve, which is important in the context of dental implant surgery.

CONFLICT OF INTEREST
Florian Andreas Probst, Josef Schweiger, Maria Juliane Stumbaum, and Monika Probst have applied for a German patent on the subject of a device and method to support imaging of MRI. Dimitrios Karampinos reports grants from Philips Healthcare outside the submitted work. Egon Burian declares no conflict of interest.

ORCID
Florian Andreas Probst https://orcid.org/0000-0002-0261-2030

REFERENCES
1. Jacobs R, Salmon B, Codari M, Hassan B, Bornstein MM. Cone beam computed tomography in implant dentistry: recommendations for clinical use. *BMC Oral Health*. 2018;18(1):88.
2. Tahmaseb A, Wu V, Wismeijer D, Coucke W, Evans C. The accuracy of static computer-aided implant surgery: a systematic review and meta-analysis. *Clin Oral Implants Res*. 2018;29(Suppl 16):416-435.
3. Wismeijer D, Joda T, Flugge T, et al. Group 5 ITI consensus report: digital technologies. *Clin Oral Implants Res*. 2018;29(Suppl 16):436-442.
4. Zhou W, Liu Z, Song L, Kuo CL, Shafer DM. Clinical factors affecting the accuracy of guided implant surgery—a systematic review and meta-analysis. *J Evid Based Dent Pract*. 2018;18(1):28-40.
5. De Felice F, Di Carlo G, Saccucci M, Tombolini V, Polimeni A. Dental cone beam computed tomography in children: clinical effectiveness and cancer risk due to radiation exposure. *Oncology*. 2019;96(4):173-178.
6. Wu TH, Lin WC, Chen WK, Chang YC, Hwang JJ. Predicting cancer risks from dental computed tomography. *J Dent Res*. 2015;94(1):27-35.
7. Ludlow JB, Timothy R, Walker C, et al. Effective dose of dental CBCT—a meta analysis of published data and additional data for nine CBCT units. *Dentomaxillofac Radiol*. 2015;44(1):20140197.
8. Agbaje JO, de Casteele EV, Salem AS, Anumendem D, Lambrichts I, Politis C. Tracking of the inferior alveolar nerve: its implication in surgical planning. *Clin Oral Investig*. 2017;21(7):2213-2220.
9. Gray CF, Redpath TW, Smith FW. Pre-surgical dental implant assessment by magnetic resonance imaging. *J Oral Implantol*. 1996;22(2):147-153.
10. Gray CF, Redpath TW, Smith FW, Staff RT. Advanced imaging: magnetic resonance imaging in implant dentistry. *Clin Oral Implants Res*. 2003;14(1):18-27.
11. Hassfeld S, Fiebach J, Widmann S, Heiland S, Muhling J. Magnetic resonance tomography for planning dental implantation. *Mund Kiefer Gesichtschir*. 2001;5(3):186-192.
12. Pompa V, Galasso S, Cassetta M, Pompa G, De Angelis F, Di Carlo S. A comparative study of magnetic resonance (MR) and computed tomography (CT) in the pre-implant evaluation. *Ann Stomatol (Roma)*. 2010;1(3–4):33-38.
13. Flugge T, Hovener JB, Ludwig U, et al. Magnetic resonance imaging of intraoral hard and soft tissues using an intraoral coil and FLASH sequences. *Eur Radiol*. 2016;26(12):4616-4623.
14. Ludwig U, Eisenbeiss AK, Scheifele C, et al. Dental MRI using wireless intraoral coils. *Sci Rep*. 2016;6:23301.
15. Prager M, Heiland S, Gareis D, Hilgenfeld T, Bendszus M, Gaudino C. Dental MRI using a dedicated RF-coil at 3 tesla. *J Craniomaxillofac Surg*. 2015;43(10):2175-2182.
16. Assaf AT, Zrnc TA, Remus CC, et al. Evaluation of four different optimized magnetic-resonance-imaging sequences for visualization of dental and maxillo-mandibular structures at 3 T. *J Craniomaxillofac Surg*. 2014;42(7):1356-1363.
17. Hilgenfeld T, Prager M, Heil A, et al. PETRA, MSVAT-SPACE and SEMAC sequences for metal artefact reduction in dental MR imaging. *Eur Radiol*. 2017;27(12):5104-5112.
18. Probst M, Richter V, Weitz J, et al. Magnetic resonance imaging of the inferior alveolar nerve with special regard to metal artifact reduction. *J Craniomaxillofac Surg*. 2017;45(4):558-569.
19. Duttenhoefer F, Mertens ME, Vizkelety J, Gremse F, Stadelmann VA, Sauerbier S. Magnetic resonance imaging in zirconia-based dental implantology. *Clin Oral Implants Res*. 2015;26(10):1195-1202.
20. Detterbeck A, Hofmeister M, Hofmann E, et al. MRI vs. CT for orthodontic applications: comparison of two MRI protocols and three CT (multislice, cone-beam, industrial) technologies. *J Orofac Orthop*. 2016;77(4):251-261.
21. Goto TK, Nishida S, Nakamura Y, et al. The accuracy of 3-dimensional magnetic resonance 3D vibe images of the mandible: an in vitro comparison of magnetic resonance imaging and computed tomography.

Oral Surg Oral Med Oral Pathol Oral Radiol Endod. 2007;103(4):550-559.

22. van Eijnatten M, Rijkhorst EJ, Hofman M, Forouzanfar T, Wolff J. The accuracy of ultrashort echo time MRI sequences for medical additive manufacturing. *Dentomaxillofac Radiol*. 2016;45(5):20150424.

23. Hilgenfeld T, Juerchott A, Deisenhofer UK, et al. In vivo accuracy of tooth surface reconstruction based on CBCT and dental MRI-A clinical pilot study. *Clin Oral Implants Res*. 2019;30(9):920-927.

24. Mercado F, Mukaddam K, Filippi A, Bieri OP, Lambrecht TJ, Kuhl S. Fully digitally guided implant surgery based on magnetic resonance imaging. *Int J Oral Maxillofac Implants*. 2019;34(2):529-534.

25. Flugge T, Ludwig U, Hovener JB, Kohal R, Wismeijer D, Nelson K. Virtual implant planning and fully guided implant surgery using magnetic resonance imaging-proof of principle. *Clin Oral Implants Res*. 2020;31(6):575-583.

26. Assaf AT, Zrnc TA, Remus CC, et al. Early detection of pulp necrosis and dental vitality after traumatic dental injuries in children and adolescents by 3-tesla magnetic resonance imaging. *J Craniomaxillofac Surg*. 2015;43(7):1088-1093.

27. Zuniga JR, Mistry C, Tikhonov I, Dessouky R, Chhabra A. Magnetic resonance neurography of traumatic and nontraumatic peripheral trigeminal neuropathies. *J Oral Maxillofac Surg*. 2018;76(4):725-736.

28. Burian E, Probst FA, Weidlich D, et al. MRI of the inferior alveolar nerve and lingual nerve-anatomical variation and morphometric benchmark values of nerve diameters in healthy subjects. *Clin Oral Investig*. 2019;24(8):2625-2634.

29. Gersing AS, Pfeiffer D, Kopp FK, et al. Evaluation of MR-derived CT-like images and simulated radiographs compared to conventional radiography in patients with benign and malignant bone tumors. *Eur Radiol*. 2019;29(1):13-21.

30. Sang YH, Hu HC, Lu SH, Wu YW, Li WR, Tang ZH. Accuracy assessment of three-dimensional surface reconstructions of in vivo teeth from cone-beam computed tomography. *Chin Med J (Engl)*. 2016;129(12):1464-1470.

31. Lee C, Jeon KJ, Han SS, et al. CT-like MRI using the zero-TE technique for osseous changes of the TMJ. *Dentomaxillofac Radiol*. 2019;49(3):20190272.

32. Gradl J, Horeth M, Pfefferle T, et al. Application of a dedicated surface coil in dental MRI provides superior image quality in comparison with a standard coil. *Clin Neuroradiol*. 2017;27(3):371-378.

33. Monch S, Sollmann N, Hock A, Zimmer C, Kirschke JS, Hedderich DM. Magnetic resonance imaging of the brain using compressed sensing—quality assessment in daily clinical routine. *Clin Neuroradiol*. 2019;30(2):279-286.

34. Gersing AS, Bodden J, Neumann J, et al. Accelerating anatomical 2D turbo spin echo imaging of the ankle using compressed sensing. *Eur J Radiol*. 2019;118:277-284.

35. Zaitsev M, Maclaren J, Herbst M. Motion artifacts in MRI: a complex problem with many partial solutions. *J Magn Reson Imaging*. 2015;42(4):887-901.

36. Hilgenfeld T, Juerchott A, Deisenhofer UK, et al. Accuracy of cone-beam computed tomography, dental magnetic resonance imaging, and intraoral radiography for detecting peri-implant bone defects at single zirconia implants-an in vitro study. *Clin Oral Implants Res*. 2018;29(9):922-930.

37. Chockattu SJ, Suryakant DB, Thakur S. Unwanted effects due to interactions between dental materials and magnetic resonance imaging: a review of the literature. *Restor Dent Endod*. 2018;43(4):e39.

38. Bover-Ramos F, Vina-Almunia J, Cervera-Ballester J, Penarrocha-Diago M, Garcia-Mira B. Accuracy of implant placement with computer-guided surgery: a systematic review and meta-analysis comparing cadaver, clinical, and in vitro studies. *Int J Oral Maxillofac Implants*. 2018;33(1):101-115.

39. Plooij JM, Maal TJ, Haers P, Borstlap WA, Kuijpers-Jagtman AM, Berge SJ. Digital three-dimensional image fusion processes for planning and evaluating orthodontics and orthognathic surgery: a systematic review. *Int J Oral Maxillofac Surg*. 2011;40(4):341-352.

40. Flugge T, Derksen W, Te Poel J, Hassan B, Nelson K, Wismeijer D. Registration of cone beam computed tomography data and intraoral surface scans—a prerequisite for guided implant surgery with CAD-/CAM drilling guides. *Clin Oral Implants Res*. 2017;28(9):1113-1118.

41. Hilgenfeld T, Kastel T, Heil A, et al. High-resolution dental magnetic resonance imaging for planning palatal graft surgery—a clinical pilot study. *J Clin Periodontol*. 2018;45(4):462-470.

42. Wanner L, Ludwig U, Hovener JB, Nelson K, Flugge T. Magnetic resonance imaging-a diagnostic tool for postoperative evaluation of dental implants: a case report. *Oral Surg Oral Med Oral Pathol Oral Radiol*. 2018;125(4):e103-e107.

43. Juerchott A, Pfefferle T, Flechtenmacher C, et al. Differentiation of periapical granulomas and cysts by using dental MRI: a pilot study. *Int J Oral Sci*. 2018;10(2):17.

44. Probst FA, Probst M, Pautke C, et al. Magnetic resonance imaging: a useful tool to distinguish between keratocystic odontogenic tumours and odontogenic cysts. *Br J Oral Maxillofac Surg*. 2015;53(3):217-222.

45. Juerchott A, Freudlsperger C, Weber D, et al. In vivo comparison of MRI- and CBCT-based 3D cephalometric analysis: beginning of a non-ionizing diagnostic era in craniomaxillofacial imaging? *Eur Radiol*. 2019;30(3):1488-1497.